High-resolution *in vivo* imaging of bone and joints: a window to microarchitecture

Piet Geusens, Roland Chapurlat, Georg Schett, Ali Ghasem-Zadeh, Ego Seeman, Joost de Jong and Joop van den Bergh

Abstract | Imaging is essential to the evaluation of bone and joint diseases, and the digital era has contributed to an exponential increase in the number of publications on noninvasive analytical techniques for the quantification of changes to bone and joints that occur in health and in disease. One such technique is high-resolution peripheral quantitative CT (HR-pQCT), which has introduced a new dimension in the imaging of bone and joints by providing images that are both 3D and at high resolution (82 μm isotropic voxel size), with a low level of radiation exposure (3–5 μSv). HR-pQCT enables the analysis of cortical and trabecular properties separately and to apply micro-finite element analysis for calculating bone biomechanical competence *in vivo* at the distal sites of the skeleton (distal radius and distal tibia). Moreover, HR-pQCT makes possible the *in vivo* assessment of the spatial distribution, dimensions and delineation of cortical bone erosions, osteophytes, periarticular cortical and trabecular microarchitecture, and 3D joint-space volume of the finger joints and wrists. HR-pQCT is, therefore, a technique with a high potential for improving our understanding of bone and joint diseases at the microarchitectural level.

Geusens, P. *et al. Nat. Rev. Rheumatol.* **10**, 304–313 (2014); published online 4 March 2014; doi:10.1038/nrrheum.2014.23

Introduction

Imaging of bone and joints is an essential part of the evaluation of diseases that affect these structures. The digital era has contributed to an exponential increase in the number of publications on noninvasive analytical techniques for the quantification of changes that occur in healthy individuals and in those with bone and joint diseases. Imaging techniques vary in methodology (being based on X-ray, magnetic resonance or ultrasound), measurable dimensions (producing either 2D or 3D images), spatial resolution, radiation exposure, acquisition time and parameters assessed (Table 1).[1] They also vary in the size of bone or joint that can be measured (small or large), the region of interest (ROI) (whole bone or parts of bone; full spine or parts of the spine; small or large joints), accuracy, precision, cost and availability. Lastly, they vary in their power to predict clinical outcomes such as fractures (in bone diseases) and function (in joint diseases). Each method has strengths and limitations in one or more of these aspects.

The advent of high-resolution peripheral quantitative CT (HR-pQCT; XtremeCT, Scanco Medical AG, Brüttisellen, Switzerland) introduced a new dimension in the imaging of bone and joints because it provides 3D images of cortical and trabecular bone with high resolution combined with low levels of radiation exposure (Figures 1 and 2). In this Review, we present the current state of the use of HR-pQCT in the evaluation of bone and joint diseases. The technical aspects of HR-pQCT are described, together with the possibilities, pitfalls, advantages and limitations of this approach. We discuss the additional value of HR-pQCT over other imaging techniques, and provide a perspective on the potential of HR-pQCT in basic research, clinical trials and daily clinical practice.

Structure of normal and diseased bone

Osteoporosis has been defined by the WHO as a generalized skeletal disease associated with both low areal bone mineral density (aBMD) and microarchitectural changes and deterioration, resulting in an increased risk of fracture.[2] Measurement of aBMD by use of dual-energy X-ray absorptiometry (DXA) has become a widely used clinical tool for the evaluation of fracture risk; however, owing to its inherent error in accuracy and reproducibility and the limitations of projecting 3D structures onto 2D images, aBMD lacks sensitivity and specificity for fracture prediction.

The use of aBMD has led to several misconceptions due to its inability to differentiate cortical from trabecular bone and to quantify bone structure, material composition or cortical porosity.[3,4] Research examining fracture prevalence as a function of aBMD confirmed that fracture risk

Department of Internal Medicine, Subdivision of Rheumatology, CAPHRI/NUTRIM, Maastricht University Medical Centre, P. Debyelaan 25, Postbus 5800, 6202 AZ, Maastricht, Netherlands (**P.G.**, **J.d.J.**, **J.v.d.B.**). INSERM UMR 1033, Université de Lyon, Hôpital E Herriot, 69437 Lyon, cedex 03, France (**R.C.**). Department of Internal Medicine, University of Erlangen-Nuremberg, Ulmenweg 18, 91054 Erlangen, Germany (**G.S.**). Department of Medicine, Austin Health, University of Melbourne, Heidelberg Repatriation Hospital, 300 Waterdale Road, Heidelberg West, Vic 3081, Australia (**A.G.-Z.**, **E.S.**).

Correspondence to: P.G. piet.geusens@scarlet.be

Competing interests
P.G. is the coordinator of clinical studies with high-resolution peripheral quantitative CT (HR-pQCT) for which Maastricht University Medical Centre received grants from Amgen, Pfizer and Will Pharma. R.C. has been a consultant, speaker, or clinical investigator with the following companies: Amgen, Bioiberica, BMS, Chugai, Lilly, Merck, Novartis, Novo, Pfizer, Servier and UCB; R.C. has no direct or indirect link to the manufacturer of HR-pQCT. A.G.-Z. is one of the inventors of StrAx1.0, an algorithm used to quantify bone microstructure. E.S. is Director of StraxCorp and one of the inventors of StrAx1.0. G.S., J.d.J, and J.v.d.B. declare no competing interests.

Key points

- High-resolution peripheral quantitative CT (HR-pQCT) enables noninvasive evaluation of bones and joints by producing high-resolution 3D images with exposure to only low levels of radiation
- The ability to measure cortical and trabecular bone density and architecture separately has enabled us to better understand changes that occur with age, differences between sexes and races, and the effects of drug treatment
- Bone involvement in rheumatic diseases of the hand joints is heterogeneous, and a growing body of evidence indicates that 3D image analysis will enable us to quantify these changes
- Fracture healing is a complex process with concomitant and subsequent changes in cortical and trabecular bone density and architecture
- Segmenting cortical and trabecular compartments requires measurement of the transitional zone between them for accurate assessment of the effects of growth, ageing, disease, and drug therapy

increases as aBMD decreases, but also demonstrated that about 50% of all fractures occur in the large proportion of the population with osteopenia (who are at modest risk of fracture) rather than the smaller fraction of the population with osteoporosis (and consequently the highest absolute risk of fracture).[5–8] Indeed, most patients with a fragility fracture do not have osteoporosis.[7] Furthermore, changes in aBMD explain only a small proportion of the reduction in vertebral fracture risk after therapy for osteoporosis.[9] Therefore, techniques to evaluate bone-related factors other than bone mineral density (BMD), such as macroarchitecture, microarchitecture and bone quality, have been developed.

Unlike DXA, quantitative CT (QCT) and peripheral QCT techniques are able to distinguish cortical from trabecular bone. *In vivo* 3D quantification of trabecular structure by HR-pQCT was introduced in the mid-1990s,[10] and enables noninvasive assessment of bone microarchitecture and better assessment of bone fragility than the imaging methods listed in Table 1. HR-pQCT, which has a nominal resolution of 82 μm, can quantify trabecular and cortical bone structure by acquiring 110 consecutive slices from the distal radius or distal tibia.[1]

HR-pQCT can assess total, cortical and trabecular true volumetric BMD (vBMD) and parametric or nonparametric bone structure parameters,[11–13] and so provide unique insights into bone quality, a key component of bone strength. At present, this method is the only approach that provides images with a spatial resolution in the range of the trabecular scale for human *in vivo* studies. Moreover, it involves exposure to low levels of radiation (<5 μSv), and has a short scan time (<3 min),[12] so it is well suited to clinical and research uses.

Population studies

In cross-sectional analyses of population-based cohorts, HR-pQCT has identified substantial age-related differences in vBMD, trabecular structure and cortical thickness in premenopausal and postmenopausal women.[12–15] These studies reported that reduced trabecular vBMD is accompanied by reduced trabecular number and thickness, together with increased trabecular separation. These differences were paralleled by an age-related decrease in cortical thickness, consistent with higher cortical porosity both at the distal radius and distal tibia.[15] These modifications accelerated after menopause, but differed at the two distal sites. Specifically, the bone volume fraction in the trabecular region tended to remain stable up to menopause and to be lower thereafter at the distal radius, whereas it decreased from early adulthood at the distal tibia.[15] For instance, among 324 white American women in a Mayo Clinic cohort, trabecular bone volume fraction at the distal radius declined by 26% between ages 20 and 90 years,[13] and in 441 women in the Canadian Multicentre Osteoporosis Study (CaMOS) the trabecular number declined by 21% and the cortical thickness decreased by 31% at the same site.[14] At the distal tibia, the magnitude of these declines was of the same order. By contrast, trabecular thickness tended to be higher before the age of 50 years than in older women, at least in the CaMOS cohort,[14] but unexpectedly the opposite was found in the Mayo Clinic cohort,[13] possibly owing to the use of a prototype version of HR-pQCT with slightly poorer resolution (89 μm). Also, the decline in trabecular indices in young adults was not replicated in another cohort, perhaps owing to small sample size (58 men and 74 women).[15]

In the Canadian cohort, the pattern of bone impairment with increasing age also differed between the

Table 1 | Comparison of *in vivo* bone and joint imaging techniques[1]

Method	Nominal resolution (μm)	Effective radiation dose (μSv)	Acquisition time (min)	Parameters assessed
Conventional 2D radiography, hand	<50	10	<1	Bone size, cortical thickness, diseases
HR 2D radiography, hand	50	<5	<1	Trabecular structure, erosions
Adult DXA	1,000–2,500	5–20	<1	BMC, BMD
Musculoskeletal ultrasonography	200–500	0	>10	Synovitis, effusion, erosions, vascularization
MRI	150–200	0	10–30	BME, erosions, cartilage, effusion
3D QCT, spine 3D QCT, hip 3D QCT, wrist 3D HR-pQCT	250–300 250–300 250–300 82	1,500 2,900 <10 3–5	<1 <1 <1 3	BMD, cortical and trabecular structure, FEA

Abbreviations: BMC, bone mineral content; BMD, bone mineral density; BME, bone marrow oedema; DXA, dual-energy X-ray absorptiometry; FEA, finite element analysis; HR, high resolution; QCT, quantitative CT.

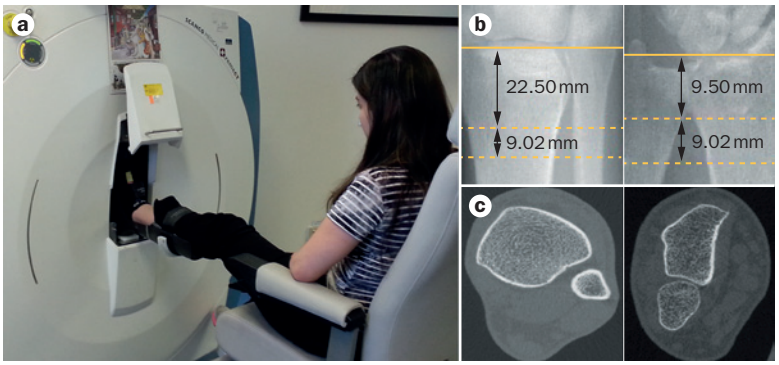

Figure 1 | HR-pQCT. **a** | Positioning of the patient on a HR-pQCT machine to scan the distal tibia. **b** | Identifying the scanning region (between the pair of dotted lines) in the tibia (left) and radius (right). **c** | Axial images of a tibia (left) and radius (right). Abbreviation: HR-pQCT, high-resolution peripheral quantitative CT.

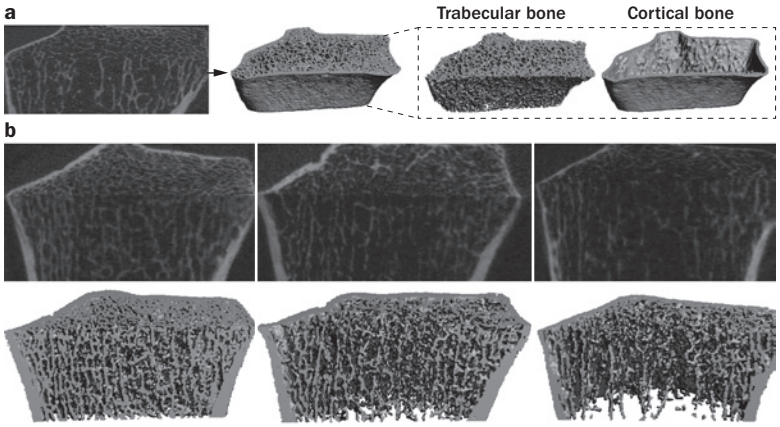

Figure 2 | Imaging of cortical and trabecular compartments with HR-pQCT. **a** | Segmentation of forearm cortical and trabecular bone in HR-pQCT images. **b** | Cortical and trabecular deterioration with ageing in the ultra-distal radius; greyscale (top) and segmented bone versus non-bone (bottom) 3D images. Abbreviation: HR-pQCT, high-resolution peripheral quantitative CT.

cortical and the trabecular compartments.[14] Cortical BMD at the radius remained fairly stable until the menopausal transition and declined thereafter; nonetheless, the proportion of load carried by the cortex remained constant over time.[14] The maximum increase in cortical porosity at the radius probably occurs between the ages of 50 and 60 years.[16] At the distal tibia, the decline in cortical BMD started before the menopausal transition.[13–15] These observations, however, were made in cross-sectional studies. The exact pattern of age-related bone loss needs to be confirmed in longitudinal analyses (Figure 2).

These cross-sectional analyses,[12–15] performed with a noninvasive technique, have confirmed the pattern of bone decline with age that was observed in past cross-sectional histomorphometric studies.[17] They also permit one to distinguish the trabecular and cortical compartments (Figure 2a), which is not possible with the measurement of aBMD provided by DXA. So far, HR-pQCT has been the only technique to enable the noninvasive evaluation of microarchitecture *in vivo*. Therefore, this technique has also the potential to better explore the morphological differences of bone fragility between men and women, between ethnic groups and also among the various forms of secondary osteoporosis (for example, in chronic renal failure and in corticosteroid-treated patients).

Patients with fractures

As aBMD determined by DXA predicts only half of fragility fractures,[18] which are observed mainly in women with aBMD in the osteopenic range, studying microarchitecture with HR-pQCT might avoid some of the intrinsic limitations of DXA. Indeed, in a case–control analysis of HR-pQCT in the French population-based OFELY cohort, osteopenic women with fragility fractures ($n = 35$) had lower trabecular density (–12.3%, $P = 0.018$) and more heterogeneous trabecular distribution (25.6%, $P = 0.011$) than women without fractures ($n = 78$) who had the same aBMD at the spine and hip.[12] Similarly, in a case–control study enrolling postmenopausal women with recent wrist ($n = 50$) or hip fractures ($n = 62$), HR-pQCT measures, in particular the cortical parameters at the distal tibia, were able to distinguish between women with fractures and healthy controls ($n = 54$).[19] Moreover, vertebral fractures in postmenopausal women have been associated with low vBMD and architectural alterations of both trabecular and cortical bone, as identified using HR-pQCT.[20] In this study, severe and multiple vertebral fractures were associated with more extensive alterations of cortical bone, with an age-adjusted odds ratio (OR) of 2.04 (95% CI, 1.02–4.00) for each SD decrease of cortical thickness, after adjustment for aBMD.

Mechanical testing of *ex vivo* bone samples is considered as the gold standard to determine bone strength, but this technique cannot be applied *in vivo*. Bone mechanical properties can be estimated using CT images, by modelling discrete 3D parts of the images (finite elements), to approach these mechanical properties without formal *ex vivo* mechanical testing. With HR-pQCT, one can estimate bone stiffness (resistance to deformation) and bone strength (the breaking capacity) by using micro-finite element analysis (μFEA). Thus, in a case–control study among postmenopausal women ($n = 66$), the proportion of load carried by cortical bone compared with trabecular bone was associated with wrist fracture independently of aBMD and microarchitecture.[21] In another cross-sectional analysis, μFEA parameters evaluated at distal sites such as the tibia and radius were also associated with all types of prevalent fractures, including vertebral fractures, and the magnitude of the association was similar at the tibia and radius.[22] Thus, at the radius, vertebral fractures were associated with trabecular microarchitecture with an OR of 1.86 (95% CI 1.14-3.03), whereas nonvertebral fractures were associated with bone strength and quantity, with an OR of 2.03 (95% CI 1.36–3.02). At the tibia, both vertebral fracture (OR = 2.92, 95% CI 1.14–3.03) and nonvertebral fracture (OR = 2.64, 95% CI 1.63–4.27) were associated with bone strength and quantity.[22] So, mechanical properties of the tibia and radius seem to be reasonably representative of those of other, distant bone sites. Local topological analysis describing rod-like and plate-like trabeculae, which is feasible with HR-pQCT at the resolution of 82 μm, might also be helpful to improve fracture risk

prediction.[23] Most of these results observed in retrospective studies were obtained after adjustment for aBMD at the radius for radius measurements and for aBMD at the hip for tibia measurements. To better establish the value of HR-pQCT in predicting fractures independently from or in combination with aBMD, prospective studies are needed.

The compartment-specific analyses that can be conducted with HR-pQCT are helpful for clarifying discrepancies between fracture prevalence and risk prediction based on aBMD. Indeed, in individuals with smaller bones, aBMD underestimates the bone density.[24] Furthermore, bone geometry and microarchitecture can be quite different at the same level of aBMD,[24] and thus these variations are not captured by the evaluation of aBMD. For instance, Asian individuals have lower aBMD but nonetheless sustain fewer fractures than white individuals with lower aBMD.[25,26] Using HR-pQCT, Wang *et al.*[27] observed that premenopausal Asian women have thicker cortices and thicker but fewer trabeculae than white women. In Chinese-American women, higher estimates of bone stiffness and strength in μFEA could thus explain why Asian individuals sustain fewer fractures than expected given they have smaller bones.[28] Moreover, in Chinese-American premenopausal and postmenopausal women, cortical porosity has been found to be lower than in white women.[29] These sort of measurements, however, can be challenging to obtain because of the difficulties in reproducing scan positioning. These difficulties can be overcome by standardizing patient positioning and carefully monitoring scan quality.

HR-pQCT has also been used to address bone fragility in men and sex-related differences in characteristics such as bone microarchitecture and size. For example, Khosla *et al.*[13] found that trabecular bone volume fraction and thickness were significantly higher in 19 young men than in 17 young women (26%, $P = 0.001$ and 28%, $P < 0.001$ respectively). The rate of age-related decline in trabecular bone volume fraction seemed to be independent of sex; however, in ageing but otherwise healthy men, trabecular thinning seemed to predominate over actual loss of trabeculae, in contrast to what is observed in women. In addition, μFEA estimates of bone strength at the distal radius and tibia in 185 men with prevalent fracture and 185 healthy individuals have been associated with prevalent fracture risk at distant sites,[22] which is reminiscent of the findings in postmenopausal women. However, men seem to experience a lesser increase in cortical porosity (84% versus 176%) and more periosteal expansion (28% versus 11% at the radius) than women.[14] Of note, these differences are probably acquired in early adulthood, because peripubertal and postpubertal girls have greater cortical density and lower cortical porosity than peripubertal and postpubertal boys.[30] In a cross-sectional analysis of 920 older men, the microarchitecture impairment seemed to be associated more with the severity of prevalent fracture than with the fracture events themselves, with ORs ranging from 1.25 to 1.94 for the association between fracture severity and the various microarchitecture parameters.[31]

Fracture healing

Fracture healing is a complex process involving many concomitant and subsequent cellular and biochemical processes. Haematoma formation, inflammation, bone repair with formation of a soft and hard callus by intramembranous and endochondral bone formation, and bone remodelling are all aspects of the healing process.

The evaluation of bone healing is one of the most difficult tasks for orthopaedic and trauma surgeons and is based on clinical findings and interpretation of conventional radiography. Such findings are subjective, and their validity in quantifying fracture healing and bone strength has been questioned.[32–35] Radiographic evidence of callus formation is dependent on the bone involved and the type and environment of the fracture.[36] Cortical bone fractures start healing periosteally and endosteally, producing ample callus, whereas metaphyseal fractures, such as stable distal radius fractures, tend to heal endosteally, with new bone being formed on existing trabeculae, producing less callus and less perceptible cortical bridging.[37,38]

With the introduction of conventional QCT, vBMD evaluation and improved 3D diagnostic evaluation of fractures became available.[39–41] CT-based imaging enabled the presence or absence cortical union in scaphoid fractures to be observed,[40] but CT was not substantially better than conventional radiography at determining healed distal radius and fibular fractures.[42]

Only a few studies using conventional QCT in animals for assessment of the fracture healing process and the evaluation of bone strength during healing have been reported. QCT-determined vBMD was strongly associated with torsional and indentation stiffness in one such study,[43] and vBMD at the fracture site was reported to be the best predictor of mechanical biomechanical competence.[44] Not surprisingly, bone structure was not assessed in either study owing to the limited resolution of clinical QCT.

The availability of HR-pQCT imaging has made it possible to measure bone structure in peripheral fractures in great detail. Mueller *et al.*[45] reported a first clinical case of a patient with a fracture at the distal radius that was treated with a new bone graft substitute. They concluded that HR-pQCT-based μFEA shows a high potential to quantify bone healing in patients.

In a pilot study presented at the American Society for Bone and Mineral Research meeting in 2012, the *in vivo* changes in bone structure and biomechanical competence at the site of fracture were analysed in 18 postmenopausal women with a stable distal radius fracture.[46] Substantial changes were detected in concomitant bone loss and gain and in stiffness at the fracture site during the healing process (Figure 3). Although promising, the application of HR-pQCT for the evaluation of fracture healing has to be further studied and validated before it can be applied to clinical practice, and will be limited to distal radius and tibia fractures.

Diseases

HR-pQCT can be used to provide insights into alterations in BMD and bone architecture in various diseases.

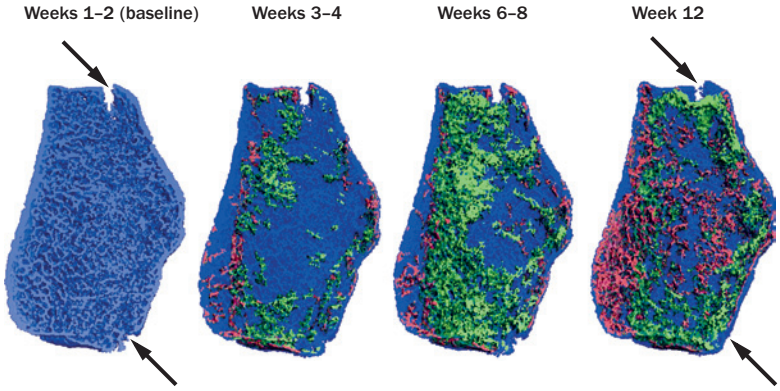

Figure 3 | HR-pQCT image showing bone apposition (green) and resorption (red) during fracture healing.[46] Images obtained by superposition of consecutive images over the baseline image. Arrows indicate cortical fracture locations. Image provided courtesy of P. Geusens and J. van den Bergh. Abbreviation: HR-pQCT, high-resolution peripheral quantitative CT.

For example, patients with type 2 diabetes mellitus typically have normal to high aBMD, but they sustain more fractures than nondiabetic controls. With HR-pQCT, it has been shown that this elevated risk could be attributable to increased cortical porosity.[47] The explanation for this increased porosity remains elusive, but it could be targeted in future clinical trials testing the value of potent antiresorptive therapies. Patients with chronic kidney disease (CKD) are at increased risk of hip and vertebral fracture.[48] In this setting, a compartment-specific approach is probably preferable to DXA, as DXA is a poor predictor of fracture and renal osteodystrophy affects trabecular and cortical compartments differently. Indeed, impaired bone microarchitecture has been observed in studies of 91 and 70 patients with early CKD[49,50] and in 79 patients on dialysis,[51] with the latter study also showing that peritoneal dialysis seemed to be less deleterious for the bone than haemodialysis.

Among 27 women with primary hyperparathyroidism compared with 27 age-matched healthy controls, no impairment was observed at the distal tibia, whereas decreased cortical and trabecular volumetric densities at the radius were found, together with reduced cortical thickness and increased cortical porosity.[52] These findings suggest that the anabolic effect of parathyroid hormone (PTH) on bone depends on mechanical loading, which is in line with what has been observed in animal models examining the influence of PTH on bone.[52] In men with chronic obstructive pulmonary disease, fat-free-mass index and gas-transfer capacity of the lung were associated with bone stiffness and failure load at the distal tibia after adjustment for femoral-neck aBMD.[53] This finding is suggestive of an influence of chronic anoxia and impaired body composition on bone health, which could not be detected with DXA; HR-pQCT might therefore become a useful tool to increase understanding of the role of lung disease in bone loss and to predict fracture in patients with chronic obstructive pulmonary disease.

In the future, HR-pQCT will probably be helpful to explore the pathophysiology of the bone deterioration that is observed in various chronic diseases, because of its ability to distinguish the cortical and trabecular bone compartments—which might be affected in different ways that are not detected by DXA—and also because of the possibility to estimate bone strength by μFEA.

Effect of antiosteoporotic drugs

So far, the effects of antiosteoporotic drugs on HR-pQCT parameters have been tested in randomized controlled trials with four classes of agent: oral bisphosphonates, denosumab, strontium ranelate and odanacatib.

Among 324 postmenopausal women randomly allocated to receive either placebo or risedronate at a dose of 35 mg per week, no differences were observed in trabecular and cortical HR-pQCT parameters between the groups at 12 months.[54] However, compared with placebo, risedronate tended to prevent decline from baseline in vBMD and cortical thickness at the distal tibia.[54] The effect of risedronate on microarchitecture was greater among women who were in the early phase of the menopause than in older women. Similarly, in a trial examining the effect of oral ibandronate at a dose of 150 mg per month compared with placebo, Chapurlat *et al.*[55] found no differences in trabecular and cortical parameters at the radius between groups, with up to 24 months of follow-up. At the tibia, however, cortical vBMD and thickness were greater in the ibandronate group than in the placebo group (2% and 5% respectively, $P<0.005$). Similarly, in a pilot trial comparing alendronate with placebo over 24 months in 53 postmenopausal women,[56] HR-pQCT measures showed improvement compared with baseline values only at the distal tibia in alendronate-treated patients. In another double-blind pilot study, 247 postmenopausal women were randomly allocated to receive denosumab (60 mg subcutaneously every 6 months), alendronate (70 mg orally every week) or placebo for 12 months.[57] In the placebo group, microarchitecture variables declined; in the alendronate group, the decay was prevented; and in the denosumab group, these HR-pQCT parameters either remained stable or improved.

Strontium ranelate has been compared with alendronate in a randomized trial, but not with placebo.[58] At the radius, most comparisons were not significantly different. At the tibia, parameters (including estimates of bone strength) remained stable in the alendronate group, whereas they improved in patients treated with strontium ranelate.

Odanacatib, a cathepsin K inhibitor currently in development, has also been tested in a randomized, double-blind placebo-controlled trial, using HR-pQCT of the distal radius and distal tibia.[59] A total of 214 postmenopausal women were randomly allocated to receive 50 mg oral odanacatib or placebo weekly for 2 years. Odanacatib increased cortical and trabecular vBMD and improved cortical thickness of the distal radius and distal tibia, and improved the estimated bone strength in the distal radius, compared with placebo.

Taken together, these data suggest that the distal tibia is more responsive to antiosteoporotic treatments than the distal radius. It is possible that the mechanical stimulus at this site improves the response to treatment and thus the distal tibia might be a preferred site for monitoring.

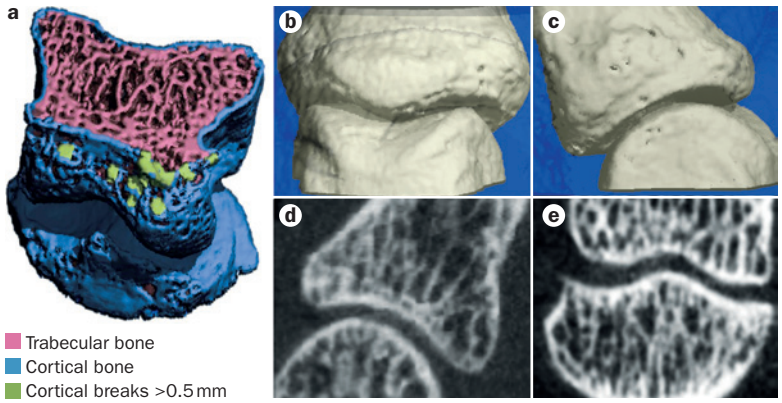

Figure 4 | HR-pQCT imaging of anatomical sites prone to develop bone erosions. **a** | 3D reconstruction of a proximal interphalangeal joint, with segmentation of cortical and trabecular bone and indication of cortical discontinuities. **b**,**c** | 3D images of the proximal interphalangeal joints in a healthy woman. **d**,**e** | Sagittal and coronal 2D images of the proximal interphalangeal joints in a healthy woman. Abbreviation: HR-pQCT, high-resolution peripheral quantitative CT.

However, as motion artefacts are especially common when measuring the radius, the scan quality has been found to be inadequate at this site in a sizeable number of cases,[60] with impairment of the reproducibility in longitudinal studies.[61] In the trials,[54–59] these inadequate scans have not been excluded, to avoid missing values and to ensure the validity of the statistical analysis. This issue might have biased some of the results towards the null, leading to the conclusion that the distal tibia site was more appropriate. Alternatively, HR-pQCT results at the radius also confirm what had already observed with aBMD and most studies of antiosteoporotic drugs; that is, the distal radius bone density is poorly responsive to therapy. Probably, the best added value of HR-pQCT in treatment evaluation is the possibility to estimate bone strength.

Imaging of joint diseases by HR-pQCT

Radiography has always been the key technique for the detection of structural bone damage in patients with inflammatory arthritis, such as rheumatoid arthritis (RA) and psoriatic arthritis (PsA). As conventional radiography is widely available, fast, cost-effective and easy to use, it has been the most feasible technique to detect and to monitor bone change in arthritis to date. Nonetheless, studies on the pathophysiology of structural bone damage in patients with arthritis, as well as investigations to exactly define the structure-protecting effect of antirheumatic therapy, might benefit from the high spatial resolution, 3D character and quantitative nature of HR-pQCT.

To date, HR-pQCT has been used to define cortical and trabecular bone changes at different anatomical sites involved in the disease processes of RA and PsA, which include the distal radius, the proximal interphalangeal joints and the metacarpophalangeal joints. HR-pQCT has enabled clinical researchers to exactly define the anatomical sites prone to develop bone erosions as well as to quantify the size of such erosions (Figure 4).[62–64] Bone erosions of >2 mm width in cortical break have been identified as highly specific for inflammatory joint diseases.[62] Whereas these large lesions are virtually absent in individuals without inflammatory joint disease, small bone erosions of <2 mm can be found frequently. Thus, up to 35% of 'healthy' individuals have small bone erosions in their phalangeal bones.[62] The pathogenesis of these lesions is unclear, but mechanical forces might be considered as the potential triggers. Furthermore, HR-pQCT has been helpful in validating the capability of other imaging techniques, such as MRI and ultrasonography, in detecting bone erosions.[65,66]

HR-pQCT has been shown to be particularly useful in monitoring the dynamics of individual bone erosions and their responsiveness to treatment. For instance, repair processes of existing bone erosions have been studied in a longitudinal manner and were identified in patients with RA treated with cytokine-blocking agents such as the TNF inhibitors adalimumab, certolizumab pegol, etanercept and infliximab as well as the IL-6-receptor blocker tocilizumab.[66,67]

Aside from bone erosions, HR-pQCT is also useful for visualizing early nonerosive cortical bone changes in patients with RA and anabolic bone changes in patients with PsA, and for assessing bone quality at the distal radius in patients with inflammatory arthritis. Indeed, in patients with RA, areas of the periarticular bone where the cortical lining is thin and porous (cortical fenestration) have been defined by HR-pQCT.[61] Most importantly, such lesions have also been identified in patients with RA-specific autoantibodies against citrullinated proteins before they develop inflammatory disease.[68] These findings suggest that bone is altered by autoimmunity in patients with RA before inflammation emerges, and creates new concepts in understanding the pathogenesis of RA. Furthermore, bone anabolic changes such as the emergence of osteophytes and enthesophytes from the periarticular periosteum and the insertion sites of the tendons can be visualized using HR-pQCT. These lesions are particular prominent in PsA, and HR-pQCT enables the assessment of their localization and the quantification of their size.[69] Moreover, these lesions can be assessed in a longitudinal manner, permitting the effects of anti-rheumatic therapy in patients with PsA to be monitored.[70] Finally, two HR-pQCT studies have shown that RA is associated with marked trabecular bone loss and profound changes in the trabecular bone network in the distal radius and the phalangeal bones.[71,72] These data suggest that both cortical and trabecular bone structure is changed not only in quantity but also in quality in patients with RA, reflecting the burden of inflammation on the bone and explaining the substantial increase in fracture risk of RA patients.

Possibilities and pitfalls of HR-pQCT

The development of HR-pQCT is an important advance in bone image acquisition and analysis. HR-pQCT can be used to investigate the structural basis of the attainment of peak bone strength during growth,[73] the structural basis of age-related and menopause-related deterioration in bone strength,[14] sex-associated and racial differences in bone structure,[27,74] arthritis-related bone changes,[62–64] and the effects of drug therapy on bone structure.[75] However,

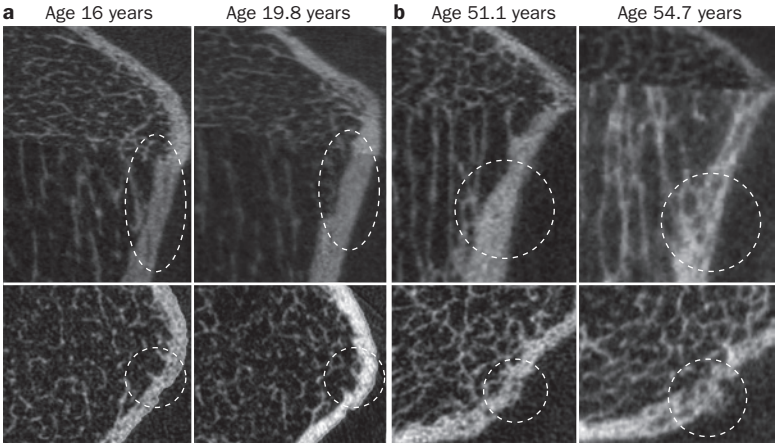

Figure 5 | HR-pQCT images showing increment and decline of cortical and trabecular vBMD during growth and ageing. **a** | 2D (lower panel) and 3D (upper panel) greyscale images of the tibia of an Asian man, showing the increase in total and cortical vBMD and cortical thickness between the ages of 16 and 19.8 years. **b** | 2D (lower panel) and 3D (upper panel) greyscale images of the tibia of a white woman, showing the decrease in total and cortical vBMD and the increase in cortical porosity between the ages of 51.1 and 54.7 years. Abbreviations: HR-pQCT, high-resolution peripheral quantitative CT; vBMD, volumetric bone mineral density.

the method has limitations that might result in misleading information if not recognized.

Identifying the transitional zone

Current image-analysis programmes segment bone compartments using thresholding, and assume bone has two compartments (cortical and trabecular). However, in any location containing both cortical and trabecular bone (such as the femoral neck), including metaphyses and short bones (such as vertebrae), a transitional or corticotrabecular zone is also present, comprising cortical bone and trabeculae abutting the endocortical surface.[76]

The distinction between the two types of bone can be difficult, and this issue might produce errors in quantifying cortical and trabecular morphology during advancing age and drug therapy. For example, vigorous intracortical remodelling results in porosity and cortical fragments that resemble trabeculae.[77] Furthermore, periarticular cortical bone is thinner and more porous than other cortical regions, making distinction between trabecular and cortical bone challenging at this location. Indeed, thresholding might apportion the porosity and the cortical fragments to the medullary compartment, erroneously elevating trabecular density and thus underestimating the age-related loss of trabecular bone, the rise in cortical porosity with age and the cortical bone volume in old age (as it is 'seen' as trabecular bone). Moreover, the transitional zone is not quantified using current HR-pQCT software (Figure 5).[78]

This issue is addressed by the development of new software that analyses images using a non-threshold-based algorithm (known as StrAx1.0), which assigns the voxel contents according to their anatomical location. This method segments compact-appearing cortex, outer and inner transitional zones, and medullary compartments, enabling a more accurate assessment of morphology, including cortical porosity below, as well as above, 100 μm in diameter.[78]

Effects of thresholding on trabecular indices

At the resolution of HR-pQCT, trabeculae span 1–2 voxels, resulting in partial volume effects if thresholding is used, as soft tissue is included in the voxel volume. The attenuation produced could be below the threshold designated as 'trabecular' bone and might therefore compromise accuracy.

The HR-pQCT software directly measures the trabecular number as the inverse of the mean distance between the mid-axes of the trabeculae. The mean distance between these axes is calculated using 3D distance transformation.[11,79] Trabecular thickness and separation are then derived using the trabecular bone volume fraction and the trabecular number.[11] Hence, the trabecular thickness and separation are dependent on trabecular number and trabecular bone volume fraction. Cortical remnants that resemble trabeculae might be included in these calculations, thus resulting in an underestimation of the decline in trabecular thickness with age or in disease states. The accuracy of other indices, such as structural model index, connectivity density and degree of anisotropy, depends on the resolution of the images, such that the latter two parameters might be underestimated at the resolution of 82 μm.[80] Furthermore, standard software to assess trabecular parameters in regions other than the distal radius, such as the metacarpal heads, is not currently available.

Issues in selection of a region of interest

The settings for scanning the ultra-distal radius or tibia use the endplate as a reference, selecting a ROI 9.5 mm and 22.5 mm proximally to the endplate of the radius and the tibia, respectively.[12,27,73] In growing children, this fixed distance becomes more distal as the bone lengthens. Moreover, the tibia grows more at its proximal than distal metaphysis, whereas the radius grows more at its distal metaphysis, so the changes and errors are likely to differ by region.[73] Errors might occur when comparing sexes or races, and taller and shorter individuals, as the fixed ROI is automatically placed more distally in those with longer limbs. The cortex might be thinner and more porous and the trabecular content higher in these individuals. Scanning a region located at a set percentage of the total bone length by adjusting the ROI is therefore recommended, but further work is needed to address this challenge.[73,81]

'Slice matching' in longitudinal studies

Site-specific variations along the length of the bone might result in errors. For example, if the ROI is positioned 0.5 mm from the previous scan it results, on average, in a 2% and 6% error in the tibial and radial vBMD, respectively.[82] The HR-pQCT software matches slices derived from consecutive images by matching their total cross-sectional areas. Finding exact slices by this method is problematic when therapy influences bone size, for example in the case of periosteal apposition. Site selection

by size will obscure periosteal apposition: if there is indeed periosteal apposition, a different ROI will be measured. Thus, new approaches to image registration are needed. In a 2013 study, Valentinitsch *et al.*[83] developed a computational trabecular clusters identification method, which is a new post-processing algorithm to quantify microarchitecture characteristics by analysing texture features in HR-pQCT images. This technique potentially can be used to find out same ROI on HR-pQCT images.

Beam hardening

Beam hardening is the process of increasing the average energy level of an X-ray beam by filtering out the low-energy photons. For example, if the cortex is thick, beam hardening will be augmented and thus the residual high-energy photon beam will be less attenuated by the adjacent trabecular bone than a beam that has travelled through a thin cortex, thus introducing errors in the estimation of trabecular morphology. Therefore, it is important to use filters and beam-hardening correction factors to take these potential sources of error into consideration.[84]

Other limitations

HR-pQCT scans are limited to the distal radius and distal tibia. Midshaft measurements cannot be performed because of the design of the HR-pQCT device. Moreover, owing to feasibility issues, assessment of periarticular bone is confined to certain predefined joint regions rather than assessment of the entire hand. Reproducibility errors are low for vBMD (0.7–1.5%), but for trabecular indices they are 3–5%,[12,60,85] and the reproducibility of these indices is unknown when they are evaluated more distally or proximally to the default ROI.

Although the image acquisition time is <3 min, movement of the patient during scanning is common and results in poor quality images, particularly of the radius, and rescanning is needed in ~30% of patients.[86] In the blurred images, trabecular indices and cortical porosity are likely to be particularly prone to error compared with densitometric indices owing to the partial volume effect.[86] When performing longitudinal studies, special care must be applied to control patient motion,[25] and in multicentre studies the study design has to account for variability across different imaging centres and phantom-based multicentre precision values need to be evaluated.[85]

The results of interventions should be interpreted with caution. Mineralization of bone is a dynamic process, in which newly formed unmineralized collagen is mineralized progressively, only reaching full mineralization after 6–12 months. The more resorption is suppressed, the longer the time available to achieve maximal mineralization—that is, secondary mineralization.[87] In addition, in the case of strontium ranelate, the high attenuation caused by this agent can increase voxel density even in the absence of new bone formation or mineralization.[58] Indeed, when corrected with parameters less influenced by density, using a distance transformation method, differences observed between patients treated with alendronate and those given strontium ranelate were not statistically significant.[58]

Technical limitations also exist in the longitudinal evaluation of cortical thickness. The analyses that have been conducted so far were limited to geometrical and microarchitectural responses to therapy, and did not address the issue of bone material effects. Moreover, the common ROI between baseline and follow-up scans is determined on the basis of cross-sectional area matching, assuming a constant area over time. Therefore, the total areas are necessarily the same when measured longitudinally. The increase in vBMD following the decrease in bone resorption can influence edge detection, artificially increasing the cortical area and thickness. In fact, the increase in cortical BMD leading to apparent improvement in cortical thickness is likely to be due to filling of cortical porosity—increasing the cortical area—because any real thickening is beyond the resolution of HR-pQCT. This hypothesis is supported by Chapurlat *et al.*,[55] who observed that the trabecular area decreased and the cortical area increased at the tibia in patients on ibandronate compared with those taking placebo, although the total area remained constant over time, suggesting that the greater cortical thickness was due to refilled endocortical porosity.

One of the limitations when using HR-pQCT techniques to evaluate fracture healing is the low radio-opacity of cartilage that is formed at the early stages of the healing process. However, a 2013 paper by Hayward *et al.*[88] reported a contrast-enhanced CT method for providing accurate and non-destructive visualization of the fracture callus, even during the early stages of repair when little mineralized tissue is present. Although the evaluation of fracture healing might benefit from the use of contrast-enhanced CT, this method is currently limited to animal studies.

Finally, HR-pQCT is unable to provide information concerning material properties such as mineral-to-matrix ratio, crystal size, collagen type and microdamage. Other modalities, such as synchrotron, electron microscopy, nanoindentation or Fourier-transform infrared spectroscopy, are required; however, these techniques are not available for *in vivo* studies.

Suggestions for the future of HR-pQCT

Future developments in HR-pQCT technology might provide additional potential for bone imaging. For example, improving the resolution of HR-pQCT images will overcome limitations in accurately quantifying the trabecular structure, but this enhancement might be at the cost of exposure to higher doses of radiation. Other improvements to the HR-pQCT system in future, such as shorter scanning times and the ability to scan the midshaft of the radius or tibia, might provide insights into cortical geometrical changes in growing children.

Conclusions

A wealth of data is emerging through the use of HR-pQCT in bone and joint research, in normal and pathological conditions. In the field of bone, we are now starting to better understand the separate behaviour of the cortical and trabecular bone compartments during normal life, in patients with fractures, in other bone diseases and during fracture healing. In joint diseases of the hand, HR-pQCT

will enable us to better understand the bone involvement in RA, PsA and hand osteoarthritis in terms of the degree and sequence of destruction and formation of cortical and trabecular bone, and to evaluate 3D cartilage volumes. In fracture healing, major changes in cortical and trabecular bone have been identified, and further studies will enable us to better understand these changes in relation to clinical outcome during fracture healing. However, several pitfalls remain to be overcome, to define the role of HR-pQCT in basic clinical research and in the study of interventions in bone and joint diseases.

Review criteria

ISI and PubMed databases were searched for published original articles that were related to the imaging of bone. Search terms included "bone", "fracture healing" and "rheumatoid arthritis" in combination with "HR-pQCT" or "HRpQCT". Manuscripts reviewed were full-text and published in English. The citations from these articles were also used to identify additional manuscripts of interest. The ISI citation index was used to identify highly cited articles in the field. No restrictions were placed on the publication date. The reference list was last updated in October 2013.

1. Link, T. M. Osteoporosis imaging: state of the art and advanced imaging. *Radiology* **263**, 3–17 (2012).
2. Kanis, J. A. Assessment of fracture risk and its application to screening for postmenopausal osteoporosis: synopsis of a WHO report. WHO Study Group. *Osteoporos. Int.* **4**, 368–381 (1994).
3. Seeman, E. Clinical review 137: Sexual dimorphism in skeletal size, density, and strength. *J. Clin. Endocrinol. Metab.* **86**, 4576–4584 (2001).
4. Nicks, K. M. *et al.* Relationship of age to bone microstructure independent of areal bone mineral density. *J. Bone Miner. Res.* **27**, 637–644 (2012).
5. Sanders, K. M. *et al.* Half the burden of fragility fractures in the community occur in women without osteoporosis. When is fracture prevention cost-effective? *Bone* **38**, 694–700 (2006).
6. Schuit, S. C. *et al.* Fracture incidence and association with bone mineral density in elderly men and women: the Rotterdam Study. *Bone* **34**, 195–202 (2004).
7. Siris, E. S. *et al.* Bone mineral density thresholds for pharmacological intervention to prevent fractures. *Arch. Intern. Med.* **164**, 1108–1112 (2004).
8. Langsetmo, L. *et al.* Repeat low-trauma fractures occur frequently among men and women who have osteopenic BMD. *J. Bone Miner. Res.* **24**, 1515–1522 (2009).
9. Delmas, P. D. & Seeman, E. Changes in bone mineral density explain little of the reduction in vertebral or nonvertebral fracture risk with anti-resorptive therapy. *Bone* **34**, 599–604 (2004).
10. Müller, R., Hildebrand, T. & Rüegsegger, P. Non-invasive bone biopsy: a new method to analyse and display the three-dimensional structure of trabecular bone. *Phys. Med. Biol.* **39**, 145–164 (1994).
11. Laib, A., Häuselmann, H. J. & Rüegsegger, P. *In vivo* high resolution 3D-QCT of the human forearm. *Technol. Health Care* **6**, 329–37 (1998).
12. Boutroy, S., Bouxsein, M. L., Munoz, F. & Delmas, P. D. *In vivo* assessment of trabecular bone microarchitecture by high-resolution peripheral quantitative computed tomography. *J. Clin. Endocrinol. Metab.* **90**, 6508–6515 (2005).
13. Khosla, S. *et al.* Effects of sex and age on bone microstructure at the ultradistal radius: a population-based noninvasive *in vivo* assessment. *J. Bone Miner. Res.* **21**, 124–131 (2006).
14. Macdonald, H. M., Nishiyama, K. K., Kang, J., Hanley, D. A. & Boyd, S. K. Age-related patterns of trabecular and cortical bone loss differ between sexes and skeletal sites: a population-based HR-pQCT study. *J. Bone Miner. Res.* **26**, 50–62 (2011).
15. Dalzell, N. *et al.* Bone micro-architecture and determinants of strength in the radius and tibia: age-related changes in a population-based study of normal adults measured with high-resolution pQCT. *Osteoporos. Int.* **20**, 1683–1694 (2009).
16. Burghardt, A. J., Kazakia, G. J., Ramachandran, S., Link, T. M. & Majumdar, S. Age- and gender-related differences in the geometric properties and biomechanical significance of intracortical porosity in the distal radius and tibia. *J. Bone Miner. Res.* **25**, 983–993 (2010).
17. Meunier, P. *et al.* Physiological senile involution and pathological rarefaction of bone. Quantitative and comparative histological data. *Clin. Endocrinol. Metab.* **2**, 239–256 (1973).
18. Sornay-Rendu, E., Munoz, F., Garnero, P., Duboeuf, F. & Delmas, P. D. Identification of osteopenic women at high risk of fracture: the OFELY study. *J. Bone Miner. Res.* **20**, 1813–1819 (2005).
19. Vico, L. *et al.* High-resolution pQCT analysis at the distal radius and tibia discriminates patients with recent wrist and femoral neck fractures. *J. Bone Miner. Res.* **23**, 1741–1750 (2008).
20. Sornay-Rendu, E., Cabrera-Bravo, J. L., Boutroy, S., Munoz, F. & Delmas, P. D. Severity of vertebral fractures is associated with alterations of cortical architecture in postmenopausal women. *J. Bone Miner. Res.* **24**, 737–743 (2009).
21. Boutroy, S. *et al.* Finite element analysis based on *in vivo* HR-pQCT images of the distal radius is associated with wrist fracture in postmenopausal women. *J. Bone Miner. Res.* **23**, 392–399 (2008).
22. Vilayphiou, N. *et al.* Finite element analysis performed on radius and tibia HR-pQCT images and fragility fractures at all sites in postmenopausal women. *Bone* **46**, 1030–1037 (2010).
23. Pialat, J. B. *et al.* Local topological analysis at the distal radius by HR-pQCT: application to *in vivo* bone microarchitecture and fracture assessment in the OFELY study. *Bone* **51**, 362–368 (2012).
24. Seeman, E. Growth in bone mass and size—are racial and gender differences in bone mineral density more apparent than real? *J. Clin. Endocrinol. Metab.* **83**, 1414–1419 (1998).
25. Wang, X. F., Duan, Y., Beck, T. J. & Seeman, E. Varying contributions of growth and ageing to racial and sex differences in femoral neck structure and strength in old age. *Bone* **36**, 978–986 (2005).
26. Xu, L., Lu, A., Zhao, X., Chen, X. & Cummings, S. R. Very low rates of hip fracture in Beijing, People's Republic of China: the Beijing Osteoporosis Project. *Am. J. Epidemiol.* **144**, 901–907 (1996).
27. Wang, X. F. *et al.* Differences in macro- and microarchitecture of the appendicular skeleton in young Chinese and white women. *J. Bone Miner. Res.* **24**, 1946–1952 (2009).
28. Liu, X. S. *et al.* Better skeletal microstructure confers greater mechanical advantages in Chinese-American women versus white women. *J. Bone Miner. Res.* **26**, 1783–1792 (2011).
29. Boutroy, S. *et al.* Lower cortical porosity and higher tissue mineral density in Chinese-American versus white women. *J. Bone Miner. Res.* http://dx.doi.org/10.1002/jbmr.2057.
30. Nishiyama, K. K. *et al.* Cortical porosity is higher in boys compared with girls at the distal radius and distal tibia during pubertal growth: an HR-pQCT study. *J. Bone Miner. Res.* **27**, 273–282 (2012).
31. Szulc, P. *et al.* Cross-sectional analysis of the association between fragility fractures and bone microarchitecture in older men: the STRAMBO study. *J. Bone Miner. Res.* **26**, 1358–1367 (2011).
32. Blokhuis, T. J. *et al.* The reliability of plain radiography in experimental fracture healing. *Skeletal Radiol.* **30**, 151–156 (2001).
33. Panjabi, M. M., Lindsey, R. W., Walter, S. D. & White, A. A. 3rd. The clinician's ability to evaluate the strength of healing fractures from plain radiographs. *J. Orthop. Trauma* **3**, 29–32 (1989).
34. Davis, B. J. *et al.* Reliability of radiographs in defining union of internally fixed fractures. *Injury* **35**, 557–561 (2004).
35. Firoozabadi, R. *et al.* Qualitative and quantitative assessment of bone fragility and fracture healing using conventional radiography and advanced imaging technologies—focus on wrist fracture. *J. Orthop. Trauma* **22** (Suppl.), S83–S90 (2008).
36. Marsh, D. Concepts of fracture union, delayed union, and nonunion. *Clin. Orthop. Relat. Res.* **355** (Suppl.), S22–S30 (1998).
37. Sevitt, S. The healing of fractures of the lower end of the radius. A histological and angiographic study. *J. Bone Joint Surg. Br.* **53**, 519–531 (1971).
38. Uhthoff, H. K. & Rahn, B. A. Healing patterns of metaphyseal fractures. *Clin. Orthop. Relat. Res.* **160**, 295–303 (1981).
39. Bhattacharyya, T. *et al.* The accuracy of computed tomography for the diagnosis of tibial nonunion. *J. Bone Joint Surg. Am.* **88**, 692–697 (2006).
40. Singh, H. P. *et al.* Partial union of acute scaphoid fractures. *J. Hand Surg. Br.* **30**, 440–445 (2005).
41. Zhu, Y. *et al.* Computed tomography-based Three-Column Classification in tibial plateau fractures: introduction of its utility and assessment of its reproducibility. *J. Trauma Acute Care Surg.* **73**, 731–737 (2012).
42. Grigoryan, M. *et al.* Quantitative and qualitative assessment of closed fracture healing using computed tomography and conventional radiography. *Acad. Radiol.* **10**, 1267–1273 (2003).
43. Markel, M. D., Morin, R. L., Wikenheiser, M. A., Lewallen, D. G. & Chao, E. Y. Quantitative CT for the evaluation of bone healing. *Calcif. Tissue Int.* **49**, 427–432 (1991).
44. Augat, P., Merk, J., Genant, H. K. & Claes, L. Quantitative assessment of experimental fracture repair by peripheral computed tomography. *Calcif. Tissue Int.* **60**, 194–199 (1997).

45. Mueller, T. L. *et al.* Mechanical stability in a human radius fracture treated with a novel tissue-engineered bone substitute: a non-invasive, longitudinal assessment using high-resolution pQCT in combination with finite element analysis. *J. Tissue Eng. Regen. Med.* **5**, 415–420 (2011).
46. Bours, S. *et al.* Fracture healing in postmenopausal women with a distal radius fracture monitored by high-resolution peripheral quantitative computer tomography (HRpQCT): a pilot study [MO0056]. Presented at the ASBMR 2012 Annual Meeting.
47. Burghardt, A. J. *et al.* High-resolution peripheral quantitative computed tomographic imaging of cortical and trabecular bone microarchitecture in patients with type 2 diabetes mellitus. *J. Clin. Endocrinol. Metab.* **95**, 5045–5055 (2010).
48. Nickolas, T. L., McMahon, D. J. & Shane, E. Relationship between moderate to severe kidney disease and hip fracture in the United States. *J. Am. Soc. Nephrol.* **17**, 3223–3232 (2006).
49. Nickolas, T. L. *et al.* Bone mass and microarchitecture in CKD patients with fracture. *J. Am. Soc. Nephrol.* **21**, 1371–1380 (2010).
50. Bacchetta, J. *et al.* Early impairment of trabecular microarchitecture assessed with HR-pQCT in patients with stage II–IV chronic kidney disease. *J. Bone Miner. Res.* **25**, 849–857 (2010).
51. Pelletier, S. *et al.* Bone microarchitecture is more severely affected in patients on hemodialysis than in those receiving peritoneal dialysis. *Kidney Int.* **82**, 581–588 (2012).
52. Hansen, S., Beck Jensen, J. E., Rasmussen, L., Hauge, E. M. & Brixen, K. Effects on bone geometry, density, and microarchitecture in the distal radius but not the tibia in women with primary hyperparathyroidism: a case–control study using HR-pQCT. *J. Bone Miner. Res.* **25**, 1941–1947 (2010).
53. Romme, E. A. *et al.* Bone stiffness and failure load are related with clinical parameters in men with chronic obstructive pulmonary disease. *J. Bone Miner. Res.* **28**, 2186–2193 (2013).
54. Bala, Y. *et al.* Risedronate slows or partly reverses cortical and trabecular micro-architectural deterioration in postmenopausal women. *J. Bone Miner. Res.* **29**, 380–388 (2014).
55. Chapurlat, R. D. *et al.* Effect of oral monthly ibandronate on bone microarchitecture in women with osteopenia—a randomized placebo-controlled trial. *Osteoporos. Int.* **24**, 311–320 (2013).
56. Burghardt, A. J. *et al.* A longitudinal HR-pQCT study of alendronate treatment in postmenopausal women with low bone density: relations among density, cortical and trabecular microarchitecture, biomechanics, and bone turnover. *J. Bone Miner. Res.* **25**, 2558–2571 (2010).
57. Seeman, E. *et al.* Microarchitectural deterioration of cortical and trabecular bone: differing effects of denosumab and alendronate. *J. Bone Miner. Res.* **25**, 1886–1894 (2010).
58. Rizzoli, R. *et al.* Effects of strontium ranelate and alendronate on bone microstructure in women with osteoporosis. Results of a 2-year study. *Osteoporos. Int.* **23**, 305–315 (2012).
59. De Papp, A. *et al.* Effects of odanacatib on the distal radius and tibia in postmenopausal women: improvements in cortical geometry and estimated bone strength [presentation 1028]. Presented at the ASBMR 2012 Annual Meeting.
60. MacNeil, J. A. & Boyd, S. K. Improved reproducibility of high-resolution peripheral quantitative computed tomography for measurement of bone quality. *Med. Eng. Phys.* **30**, 792–799 (2008).
61. Pialat, J. B., Burghardt, A. J., Sode, M., Link, T. M. & Majumdar, S. Visual grading of motion induced image degradation in high resolution peripheral computed tomography: impact of image quality on measures of bone density and micro-architecture. *Bone* **50**, 111–118 (2012).
62. Stach, C. M. *et al.* Periarticular bone structure in rheumatoid arthritis patients and healthy individuals assessed by high-resolution computed tomography. *Arthritis Rheum.* **62**, 330–339 (2010).
63. Srikhum, W. *et al.* Quantitative and semiquantitative bone erosion assessment on high-resolution peripheral quantitative computed tomography in rheumatoid arthritis. *J. Rheumatol.* **40**, 408–416 (2013).
64. Barnabe, C., Szabo, E., Martin, L., Boyd, S. K. & Barr, S. G. Quantification of small joint space width, periarticular bone microstructure and erosions using high-resolution peripheral quantitative computed tomography in rheumatoid arthritis. *Clin. Exp. Rheumatol.* **31**, 243–250 (2013).
65. Albrecht, A. *et al.* The structural basis of MRI bone erosions: an assessment by microCT. *Ann. Rheum. Dis.* **72**, 1351–1357 (2013).
66. Finzel, S. *et al.* Interleukin-6 receptor blockade induces limited repair of bone erosions in rheumatoid arthritis: a micro CT study. *Ann. Rheum. Dis.* **72**, 396–400 (2013).
67. Finzel, S. *et al.* Repair of bone erosions in rheumatoid arthritis treated with tumour necrosis factor inhibitors is based on bone apposition at the base of the erosion. *Ann. Rheum. Dis.* **70**, 1587–1593 (2011).
68. Kleyer, A. *et al.* Bone loss before the clinical onset of rheumatoid arthritis in subjects with anticitrullinated protein antibodies. *Ann. Rheum. Dis.* http://dx.doi.org/10.1136/annrheumdis-2012-202958.
69. Finzel, S., Englbrecht, M., Engelke, K., Stach, C. & Schett, G. A comparative study of periarticular bone lesions in rheumatoid arthritis and psoriatic arthritis. *Ann. Rheum. Dis.* **70**, 122–127 (2011).
70. Finzel, S. *et al.* Bone anabolic changes progress in psoriatic arthritis patients despite treatment with methotrexate or tumour necrosis factor inhibitors. *Ann. Rheum. Dis.* **72**, 1176–1181 (2013).
71. Zhu, T. Y. *et al.* Structure and strength of the distal radius in female patients with rheumatoid arthritis: a case–control study. *J. Bone Miner. Res.* **28**, 794–806 (2013).
72. Fouque-Aubert, A. *et al.* Assessment of hand bone loss in rheumatoid arthritis by high-resolution peripheral quantitative CT. *Ann. Rheum. Dis.* **69**, 1671–1676 (2010).
73. Wang, Q. *et al.* Rapid growth produces transient cortical weakness: a risk factor for metaphyseal fractures during puberty. *J. Bone Miner. Res.* **25**, 1521–1526 (2010).
74. Walker, M. D. *et al.* Differences in bone microarchitecture between postmenopausal Chinese-American and white women. *J. Bone Miner. Res.* **26**, 1392–1398 (2011).
75. Seeman, E. Bone morphology in response to alendronate as seen by high-resolution computed tomography: through a glass darkly. *J. Bone Miner. Res.* **25**, 2553–2557 (2010).
76. Keshawarz, N. M. & Recker, R. R. Expansion of the medullary cavity at the expense of cortex in postmenopausal osteoporosis. *Metab. Bone Dis. Relat. Res.* **5**, 223–228 (1984).
77. Zebaze, R. M. *et al.* Intracortical remodelling and porosity in the distal radius and post-mortem femurs of women: a cross-sectional study. *Lancet* **375**, 1729–1736 (2010).
78. Zebaze, R., Ghasem-Zadeh, A., Mbala, A. & Seeman, E. A new method of segmentation of compact-appearing, transitional and trabecular compartments and quantification of cortical porosity from high resolution peripheral quantitative computed tomographic images. *Bone* **54**, 8–20 (2013).
79. Laib, A. & Rüegsegger, P. Comparison of structure extraction methods for *in vivo* trabecular bone measurements. *Comput. Med. Imaging Graph.* **23**, 69–74 (1999).
80. Sode, M., Burghardt, A. J., Nissenson, R. A. & Majumdar, S. Resolution dependence of the non-metric trabecular structure indices. *Bone* **42**, 728–736 (2008).
81. Burrows, M. *et al.* Assessing bone microstructure at the distal radius in children and adolescents using HR-pQCT: a methodological pilot study. *J. Clin. Densitom.* **13**, 451–455 (2010).
82. Boyd, S. K. Site-specific variation of bone micro-architecture in the distal radius and tibia. *J. Clin. Densitom.* **11**, 424–430 (2008).
83. Valentinitsch, A. *et al.* Computational identification and quantification of trabecular microarchitecture classes by 3-D texture analysis-based clustering. *Bone* **54**, 133–140 (2013).
84. Meganck, J. A., Kozloff, K. M., Thornton, M. M., Broski, S. M. & Goldstein, S. A. Beam hardening artifacts in micro-computed tomography scanning can be reduced by X-ray beam filtration and the resulting images can be used to accurately measure BMD. *Bone* **45**, 1104–1116 (2009).
85. Burghardt, A. J. *et al.* Multicenter precision of cortical and trabecular bone quality measures assessed by high-resolution peripheral quantitative computed tomography. *J. Bone Miner. Res.* **28**, 524–536 (2013).
86. Sode, M., Burghardt, A. J., Pialat, J. B., Link, T. M. & Majumdar, S. Quantitative characterization of subject motion in HR-pQCT images of the distal radius and tibia. *Bone* **48**, 1291–1297 (2011).
87. Boivin, G. *et al.* Influence of remodeling on the mineralization of bone tissue. *Osteoporos. Int.* **20**, 1023–1026 (2009).
88. Hayward, L. N., de Bakker, C. M., Gerstenfeld, L. C., Grinstaff, M. W. & Morgan, E. F. Assessment of contrast-enhanced computed tomography for imaging of cartilage during fracture healing. *J. Orthop. Res.* **31**, 567–573 (2013).

Author contributions

All authors made substantial contributions to all aspects of the preparation of this manuscript.